Article

Comparison of Transcriptional Signatures of Three Staphylococcal Superantigenic Toxins in Human Melanocytes

Nabarun Chakraborty [1,*,†], Seshamalini Srinivasan [1,2,†], Ruoting Yang [1], Stacy-Ann Miller [1], Aarti Gautam [1], Leanne J. Detwiler [1,2], Bonnie C. Carney [3,4,5], Abdulnaser Alkhalil [3], Lauren T. Moffatt [3,4,5], Marti Jett [1], Jeffrey W. Shupp [3,4,5,6] and Rasha Hammamieh [1]

[1] Medical Readiness Systems Biology, Walter Reed Army Institute of Research, Silver Spring, MD 20910, USA; saissesh@gmail.com (S.S.); ruoting.yang.civ@mail.mil (R.Y.); stacyann.m.miller.civ@mail.mil (S.-A.M.); aarti.gautam.civ@mail.mil (A.G.); leanne_detwiler@yahoo.com (L.J.D.); marti.jett-tilton.civ@mail.mil (M.J.); rasha.hammamieh1.civ@mail.mil (R.H.)

[2] The Geneva Foundation, Walter Reed Army Institute of Research, Silver Spring, MD 20910, USA

[3] Firefighters' Burn and Surgical Research Laboratory, MedStar Health Research Institute, Washington, DC 20010, USA; bonnie.c.carney@medstar.net (B.C.C.); abdulnaser.alkhalil@medstar.net (A.A.); lauren.t.moffatt@medstar.net (L.T.M.); jeffrey.w.shupp@medstar.net (J.W.S.)

[4] Department of Surgery, Georgetown University School of Medicine, Washington, DC 20057, USA

[5] Department of Biochemistry and Molecular & Cellular Biology, Georgetown University School of Medicine, Washington, DC 20057, USA

[6] The Burn Center, MedStar Washington Hospital Center, Washington, DC 20010, USA

* Correspondence: nabarun.chakraborty2.civ@mail.mil; Tel.: +1-301-452-8940 or +1-301-319-7363

† These authors contributed equally to this work.

Abstract: *Staphylococcus aureus*, a gram-positive bacterium, causes toxic shock through the production of superantigenic toxins (sAgs) known as Staphylococcal enterotoxins (SE), serotypes A-J (SEA, SEB, etc.), and toxic shock syndrome toxin-1 (TSST-1). The chronology of host transcriptomic events that characterizes the response to the pathogenesis of superantigenic toxicity remains uncertain. The focus of this study was to elucidate time-resolved host responses to three toxins of the superantigenic family, namely SEA, SEB, and TSST-1. Due to the evolving critical role of melanocytes in the host's immune response against environmental harmful elements, we investigated herein the transcriptomic responses of melanocytes after treatment with 200 ng/mL of SEA, SEB, or TSST-1 for 0.5, 2, 6, 12, 24, or 48 h. Functional analysis indicated that each of these three toxins induced a specific transcriptional pattern. In particular, the time-resolved transcriptional modulations due to SEB exposure were very distinct from those induced by SEA and TSST-1. The three superantigens share some similarities in the mechanisms underlying apoptosis, innate immunity, and other biological processes. Superantigen-specific signatures were determined for the functional dynamics related to necrosis, cytokine production, and acute-phase response. These differentially regulated networks can be targeted for therapeutic intervention and marked as the distinguishing factors for the three sAgs.

Keywords: superantigens; gene expression; transcriptional dynamics; staphylococcal enterotoxins; SEB; SEA; TSST-1; toxins; biological networks; clustering; functional pathways; time–course analysis; cDNA microarray; human melanocytes

1. Introduction

Staphylococcus aureus (*S. aureus*) is widely circulated in nature and carried by 25–33% of normal individuals in the anterior nares and skin [1,2]. The extreme penetrance of this bacteria and its ability to colonize skin, open wounds, and other surfaces makes it a serious threat in facilities that provide health care [3,4]. The myriad of exotoxins synthesized and secreted by *S. aureus* include the Streptococcal enterotoxins (SEs), such as SEA-SEE, SEG-SEI, SEK-SET, and SEY, and the toxic shock syndrome toxin (TSST-1). As SEA is the most common toxin in food poisoning, SEB is recognized for its potent toxicity as a biological

weapon, and TSST-1 is known for being the causative agent of lethal toxic shock [5–7], they remain the primary focus of *S. aureus* toxins research [8].

Staphylococcal enterotoxins and TSST-1 are superantigens (sAgs) that bind as an intact molecule to the major histocompatibility complex II (MHC) and interact directly with the variable region of the beta chain of T-cell receptors (TCRs) without the need for processing or presentation by the antigen presenting cells (APC). These interactions activate T-cells, resulting in massive production of cytokines and chemokines, activation-induced apoptosis, and T-cell anergy [9].

The interaction of sAgs with immune cells and the ensuing pathogenesis have been well documented [10,11]. Previous work from our lab identified a set of genes in human peripheral blood mononuclear cells (PBMCs) that were expressed as early as 2 h post-SEB treatment [11] and played important roles in tissue repair, inflammation, and increased vascular permeability. Supporting studies reported SEB-induced proinflammatory mediators contribute to vasodilation, vascular leak, and edema [12–14].

The immunologic barrier raised by the skin is a concerted effort from different cell types. Keratinocytes, melanocytes, and Langerhans cells actively contributed to the innate immune response to sAgs [15]. We presently focused on the melanocytes, which are dendritic cells of neuroectodermal origin and an integral part of the epidermis [16–18]. The dendritic nature and strategic location of melanocytes in the epidermal layer of the skin allow for an ideal milieu to interact with the extra-skin environment and build response coordination among neighboring shallow skin cells.

The immunological responses of melanocytes have been attributed to their ability to express MHC molecules and other various adhesion molecules, including intercellular adhesion molecule (ICAM)-1 and vascular cell adhesion molecule (VCAM)-1 [19–21]. In addition, melanocytes can produce several cytokines, tumor necrosis factor alpha (TNF-α), and transforming growth factor beta (TGF-β1) with potential functions in phagocytosis and antigen processing and presentation [20,22,23]. The immunomodulatory cytotoxic properties of melanocytes were highlighted in a recent in vitro study, where melanocytes were exposed to *C. albicans* infection [24]. Despite the wide coverage of melanocyte research and the increasing knowledge of their role in immune response, minimal information is available about the role of melanocytes in response to sAgs. The selection of melanocytes for the present study was further justified by the differential host-sAgs responses that were essentially determined by the significant structural differences of the three sAgs, thus affecting their interactions with the host cells [8,25]. Major findings include the toxin-specific melanocyte response dynamics enabling the distinction of toxin pathogenesis; in particular, we elucidated later-stage molecular events that could have the potential for common or customized therapeutic targets for the three toxins of choice.

2. Materials and Methods

2.1. Cell Culture and Toxin Treatment

Normal human epidermal melanocytes (NHEM) and the reagents required for culturing the cells were purchased from Clonetics® (Lonza, Walkersville, MD, USA). Cells were maintained in Melanocyte Growth Medium (MGM) BulletKit® according to the supplier's instructions (Lonza, Walkersville, MD, USA). Cell cultures were established at the recommended starting cell density of 10,000 cells per cm^2 and maintained in 150 cm^2 flasks at 37 °C and 5% CO_2 in a humidified incubator.

SEA, SEB, and TSST-1 were purchased from Toxin Technology (Toxin Technology, Sarasota, FL, USA). The toxins were diluted from the stock solution to 25 µg/mL in the MGM growth media (Lonza, Walkersville, MD, USA). On the day of the assay, the cells were treated with the appropriate amount of toxins to reach a final concentration of 200 ng/mL. The toxins were inactivated by adding TRIzol (Invitrogen, Carlsbad, CA, USA) at 0.5, 2, 6, 12, 24, and 48 h post-exposure (p.e.). As controls, untreated melanocytes were grown in parallel and harvested at the same time points. Each time point for each toxin was represented by a single culture.

2.2. RNA Isolation

Total RNA was isolated with TRIzol reagent (Invitrogen, Carlsbad, CA, USA) using the manufacturer's procedure, followed by a cleanup procedure using the RNeasy MinElute Cleanup kit (QIAGEN, Germantown, MD, USA). The integrity of the extracted RNA was assessed using the 2100 Bioanalyzer instrument (Agilent Technologies, Santa Clara, CA, USA), and RNA integrity number (RIN) values were recorded.

2.3. Transcriptomic Assay and Analysis

The dual dye microarray hybridization was carried out using the SurePrint 4 × 44 K v2 Microarray Kit (Agilent Technologies, Inc., Santa Clara, CA, USA) following the vendor's protocol. Cy-5-labelled 200 ng of purified RNA was co-hybridized with Cy-3-labelled reference RNA (Agilent Technologies, Inc., Santa Clara, CA, USA) and bound to Agilent 4 × 44 k slides (Design ID: 026652). These arrays contain 41,000 unique probes targeting 27,958 Entrez gene RNAs. Following standard protocol, overnight hybridization at 55 °C was followed by a series of washes. The slides were scanned with an Agilent DNA microarray scanner and the features were extracted using the default setting of the Feature Extraction software (Feature Extraction software v.10.7, Agilent, CA, USA). The genes that displayed transcriptomic expressions at a fold change higher than 2 (fold change ≥ 2) were selected for further analysis.

Gene expression analysis used functions available in the Bioconductor Project [26] and functional heatmap tool (https://bioinfo-abcc.ncifcrf.gov/Heatmap/ (accessed on 26 August 2021). GeneSpring v.10.1 (Agilent Technologies, Inc., Santa Clara, CA, USA) was used for data visualization. Enrichment analysis was performed using Ingenuity Pathways Analysis (IPA, QIAGEN, Inc., Germantown, MD, USA). The data from this study was submitted to GEO under accession number GSE124756.

2.4. Gene Expression Validation by Nanostring Assays

A custom NanoString panel (NanoString Technologies, Seattle, WA, USA) was designed for genes deemed functionally important for the current study. The results and discussion section justify our choice of genes listed in Table S1. Six genes—*GIGYF2*, *INO80*, *USF2*, *WDR89*, *PPIA*, and *EIF2B1*—were selected as housekeeping genes based on their stable expression levels in melanocytes [27]. We followed the standard nCounter instructions [28], a master-mix containing hybridization buffer, Reporter ProbeSet, and Capture ProbeSet (volume:volume ratio of 1:1:0.5) was prepared, of which 25 µL was added to 5 µL target RNA. The GEN2 Prep Station incubation time was set at the higher sensitivity setting (3 h) and 280 fields of view (FOV) were routinely captured. Analysis and normalization of the raw NanoString data was conducted using nSolver Analysis Software v3.0 (NanoString Technologies, Seattle, WA, USA).

3. Results

3.1. Genomic Responses to the Three Toxins Are Characterized by Unique Host Expression Patterns

Principal component analysis (PCA) of transcriptomic expression data showed time-resolved clustering patterns of melanocytes exposed to three toxins for six treatment sequels (Figure 1). PC1 and PC2 represented 21.7% and 16.1% of the total variance; thus, together, PC1 and PC2 represent nearly 38% of the total variance. Within the transcriptomic variance defined by PC1 and PC2, we found three distinct clusters for each of the toxin types. These time points emerged clustered following longitudinal trends. For example, 30 min and 2 h SEA p.e. time points clustered together, and this combination was labelled as the early treatment phase. The early treatment phase was distantly located in the PCA plot from the middle treatment phase and was defined by 6 h and 12 h SEA p.e. time points. Finally, the late treatment phase was defined by 24 h and 48 h SEA p.e. time points, which were juxtaposed in the PCA landscape and distally located from the middle phase. A hypothetical line connecting these three treatment phases showed a potential temporal trend. A very similar picture emerged from TSST-1. The genes responding to SEB

treatment, however, showed a different clustering pattern, which was more apparent in the late treatment phase of SEB. A considerable Euclidian distance was observed between 24 h and 48 h SEB p.e. Therefore, unlike SEA and TSST-1, we included 24 h SEB p.e. in the middle treatment phase along with its original two members, namely 6 h and 12 h SEB p.e. This arrangement automatically labelled 48 h SEB p.e. as the sole candidate of the SEB late-treatment phase. Interestingly, the middle-to-late treatment phases (12 h, 24 h, and 48 h) of SEA p.e. clustered closely to the middle treatment phases (6 h, 12 h, 24 h) of SEB p.e.
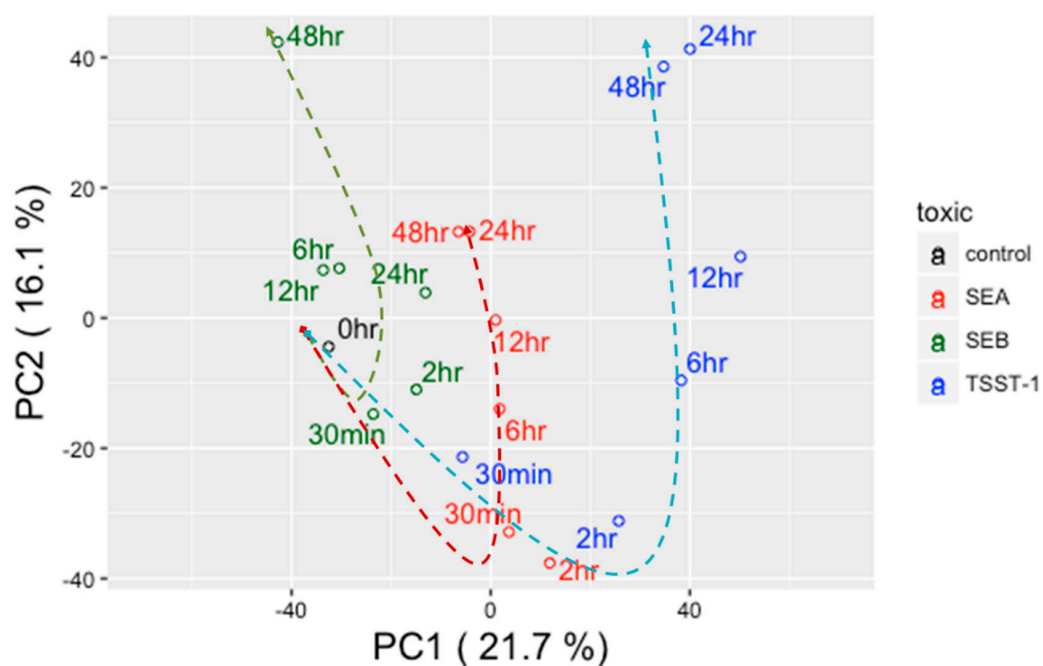

Figure 1. Principal components analysis (PCA) of time-resolved gene expression values. Black-, red-, green-, and blue-colored open circles represent control, SEA, SEB, and TSST-1, respectively. Dotted lines trace the temporal shifts caused by different toxins; here red, green, and blue dotted lines represent control, SEA, SEB, and TSST-1, respectively.

Since neither of the time point experiments have technical or biological replicates, the present strategy of grouping time sequela into the early, middle, and late treatment phases essentially enhanced the statistical confidence of the overall results. Using the longitudinal patterns of transcriptomic expressions, we sub-grouped the genes in three sets: (i) the 'Early' gene group, in which the transcriptomic fold changes were greater than |2| for at least one of the two time points (30 m and 2 h p.e.) of the early treatment phase; (ii) the 'Consistent' gene group, in which the transcriptomic fold changes were greater than |2| in all time points, and (iii) the 'Late' gene group, in which the transcriptomic fold changes were greater than |2| for at least one of the two time points (24 h and 48 h p.e.) of the late treatment phase. The exception was the SEB treatment, for which the late treatment phase included only 48 h p.e. Next, we combined (i) and (ii) to form 'Early–Consistent' gene groups; similarly, (ii) and (iii) were combined to form 'Late–Consistent' gene groups. These gene groups were used for functional analysis.

Figures S1A, S2A, and S3A depict Early–Consistent gene profiles of SEA, SEB, and TSST-1, respectively. Likewise, Figures S1B, S2B, and S3A depict Late–Consistent gene profiles of SEA, SEB, and TSST-1, respectively. A total of 445, 123, and 376 transcripts emerged, and these time clusters were called 'SEA—Early–Consistent' (SEA-E), 'SEB—Early–Consistent' (SEB–E), and 'TSST—Early–Consistent' (TSST-1-E), respectively. As explained above, the clustering for late-phase SEB exposure was performed differently than late-phase SEA and TSST-1 exposures. Hence, genes responding exclusively at 48 h p.e. (for SEB, Figure S2C) or in one of the two late p.e. phases (24 h or 48 h p.e. for SEA, Figure S1C,

and TSST-1, Figure S3C) were combined with their respective consistently expressed genes (i.e., Figure S2A for SEB, Figure S1A for SEA, and Figure S3A for TSST-1). A total of 555, 1071, and 661 genes emerged, and they were called 'SEA—Late–Consistent' (SEA-L), 'SEB—Late–Consistent' (SEB-L) and 'TSST—Late–Consistent' (TSST-1-L), respectively.

3.2. Differences in Transcriptional Regulation in Response to the Three Toxins

In agreement with the PCA trend, the number of genes showing altered transcription varied greatly in response to the three toxins (Figure S4). Comparisons of early and late genomic responses to each of the toxins showed differences that were at their maximum after SEB treatment in both up- and downregulated genes. The largest number of genes responding with fold change (FC > |2|, nearly 1100 genes) were observed in SEB-L, whereas nearly 100 genes showed FC > |2| in SEB-E. In contrast, SEA-E and SEA-L comprised the least number of genes with FC > |2|. Nearly 450 genes showed transcriptomic modulations at early time points and nearly 600 genes were modulated during the late time points. Treatment with TSST-1 toxin elicited a response somewhat like SEA p.e. Interestingly, there was a common trend among all three toxins: the number of perturbed genes increased with the progression of treatment time, indicating the transcriptomic storm typically augmented by this family of sAgs [29–32] (Figure S4).

3.3. Biological Networks and Functions That Were Differentially Regulated by the Three Toxins

Functional analysis was performed using the genes listed under SEA-E, SEA-L, SEB-E, SEB-L, TSST-1-E, and TSST-1-L, respectively, to elucidate the time-dependent, toxin-specific enrichment profiles of biological and canonical functions. Table S2 lists the top biological functions ($p < 0.001$) and canonical networks ($p < 0.01$) associated with the three early treatment categories, SEA-E, SEB-E, and TSST-1-E. The list was filtered to include only those biological processes which were significantly enriched and functionally relevant to cell survival and the defense and maintenance of skin cells. In a similar fashion, genes belonging to the late treatment phase were probed to generate a list of significant biological and canonical processes that were enriched due to the prolonged toxin exposure (Table S3).

Table 1 lists the top biological pathways ($p < 0.001$) and canonical functions ($p < 0.01$) that represent melanocytes' dendritic cell-like (DC like) or macrophage-like property. 'Antigen presentation pathways', 'dendritic cell maturation', 'IL17 signalling', and 'chemokine signalling', among others, emerged as the top functions that are related to melanocytes' immunogenicity.

ILK signalling emerged as a significant network that was conserved between the early and late treatment phases in response to all three sAg. Functional annotation of the 36 genes (Table S4) associated with the ILK signalling pathway demonstrated association with two cellular processes, namely the cell death and tight junction signalling. Other networks that responded in common to at least two toxins and were conserved throughout the time–course of the study include acute phase response signaling, the antigen presentation pathway, the complement system, and agranulocyte adhesion and diapedesis.

The Venn diagram in Figure S5A elucidated those biological networks that were common among as well as exclusive to SEA-E, SEB-E, and TSST-1-E. Nine networks related to cell survival and maintenance were affected by all three toxins. SEA-E and TSST-1-E shared the largest number (28) of networks, including those, which were associated with endometriosis, proliferation of connective tissue cells, and angiogenesis. SEA-E and SEB-E shared the smallest group of networks (2), which were related to skin disorders such as chronic skin disorder and chronic psoriasis.

A Venn diagram of the functional annotation enriched by the three late treatment phases, namely SEA-L, SEB-L, and TSST-1-L, (Figure S5B), demonstrated a cohesive picture of the early treatment phase (Figure S5A). The number of overall annotated networks was greater for the late phase (87 as compared to 66 networks for the early treatment phase), as described in Tables S2 and S3. The largest number of networks was shared between SEA-L and TSST-1-L as in the early treatment phase, with similar enriched networks, namely endometriosis and proliferation of connective tissue cells. A total of 19 networks were

commonly enriched for SEA-L and SEB-L; hence, the late treatment phase was associated with a higher number of significantly enriched gene networks than those associated with the early treatment phase.

Table 1. Biological pathways ($p < 0.001$) and canonical functions ($p < 0.01$) that represent melanocytes' dendritic cell-like (DC-like) or macrophage-like property. Networks which are perturbed by the toxins are double tick ($\sqrt{}\sqrt{}$) marked. In addition, the association of the networks with DC-like and/or macrophage-like properties are noted by single tick ($\sqrt{}$) mark.

Biological or Canonical Functions	Toxin			Biofunction Relevant to Which Melanocyte Character?	
	SEA	TSST	SEB	DC-Like	Macrophage-Like
Early					
Adhesion of blood cells	$\sqrt{}\sqrt{}$	$\sqrt{}\sqrt{}$		$\sqrt{}$	$\sqrt{}$
Antigen Presentation Pathway	$\sqrt{}\sqrt{}$	$\sqrt{}\sqrt{}$		$\sqrt{}$	$\sqrt{}$
Cdc42 Signalling	$\sqrt{}\sqrt{}$	$\sqrt{}\sqrt{}$		$\sqrt{}$	
cell movement of leukocytes	$\sqrt{}\sqrt{}$	$\sqrt{}\sqrt{}$		$\sqrt{}$	$\sqrt{}$
cell movement of phagocytes	$\sqrt{}\sqrt{}$	$\sqrt{}\sqrt{}$		$\sqrt{}$	$\sqrt{}$
Chemokine Signaling		$\sqrt{}\sqrt{}$	$\sqrt{}\sqrt{}$		$\sqrt{}$
chemotaxis of phagocytes	$\sqrt{}\sqrt{}$			$\sqrt{}$	$\sqrt{}$
Complement System	$\sqrt{}\sqrt{}$			$\sqrt{}$	$\sqrt{}$
Crosstalk between Dendritic Cells and Natural Killer Cells	$\sqrt{}\sqrt{}$			$\sqrt{}$	$\sqrt{}$
Dendritic Cell Maturation	$\sqrt{}\sqrt{}$			$\sqrt{}$	$\sqrt{}$
Differential Regulation of Cytokine Production in Macrophages and T Helper Cells by IL-17A and IL-17F	$\sqrt{}\sqrt{}$			$\sqrt{}$	$\sqrt{}$
ERK5 Signalling	$\sqrt{}\sqrt{}$				$\sqrt{}$
HMGB1 Signalling	$\sqrt{}\sqrt{}$			$\sqrt{}$	$\sqrt{}$
IL-17 Signalling	$\sqrt{}\sqrt{}$			$\sqrt{}$	$\sqrt{}$
IL-17A Signalling in Fibroblasts	$\sqrt{}\sqrt{}$			$\sqrt{}$	
IL-8 Signalling	$\sqrt{}\sqrt{}$				$\sqrt{}$
Immune response of cells	$\sqrt{}\sqrt{}$			$\sqrt{}$	$\sqrt{}$
Immune response of leukocytes	$\sqrt{}\sqrt{}$			$\sqrt{}$	$\sqrt{}$
Immune response of phagocytes			$\sqrt{}\sqrt{}$	$\sqrt{}$	$\sqrt{}$
Inflammatory response			$\sqrt{}\sqrt{}$	$\sqrt{}$	$\sqrt{}$
MAPKKK cascade			$\sqrt{}\sqrt{}$	$\sqrt{}$	$\sqrt{}$
Migration of phagocytes	$\sqrt{}\sqrt{}$			$\sqrt{}$	$\sqrt{}$
Oxidative Phosphorylation	$\sqrt{}\sqrt{}$			$\sqrt{}$	$\sqrt{}$
PDGF Signalling	$\sqrt{}\sqrt{}$				$\sqrt{}$
Proliferation of immune cells	$\sqrt{}\sqrt{}$			$\sqrt{}$	$\sqrt{}$
synthesis of prostaglandin	$\sqrt{}\sqrt{}$			$\sqrt{}$	
synthesis of prostaglandin E2	$\sqrt{}\sqrt{}$			$\sqrt{}$	

Table 1. *Cont.*

Biological or Canonical Functions	Toxin			Biofunction Relevant to Which Melanocyte Character?	
	SEA	TSST	SEB	DC-Like	Macrophage-Like
T-cell lymphoproliferative disorder	√√			√	√
Late					
Activation of blood cells	√√	√√		√	√
Adhesion of blood cells	√√	√√		√	√
Aggregation of blood cells	√√			√	√
Antigen Presentation Pathway	√√			√	√
Autophagy of cells	√√			√	√
Cell movement of connective tissue cells	√√				√
Cell movement of leukocytes	√√			√	√
Chemokine Signalling	√√			√	√
Chemotaxis of neutrophils	√√			√	√
Chemotaxis of phagocytes	√√			√	√
Complement System	√√			√	√
Crosstalk between Dendritic Cells and Natural Killer Cells	√√			√	√
Dendritic Cell Maturation	√√			√	√
Differentiation of hematopoietic progenitor cells	√√			√	√
eNOS Signalling	√√			√	√
IL-17 Signalling	√√			√	√
Immune response of cells	√√			√	√
Immune response of leukocytes	√√			√	√
Metabolism of eicosanoid	√√			√	√
Metabolism of prostaglandin			√√	√	
Migration of antigen presenting cells			√√	√	√
Migration of phagocytes			√√	√	√
Phagosome Maturation			√√	√	√
PI3K/AKT Signalling		√√		√	
Signalling by Rho Family GTPases		√√		√	√
Superoxide Radicals Degradation		√√		√	√
Synthesis of prostaglandin		√√		√	
Transmigration of phagocytes		√√		√	√

All three sAgs induced responses highly enriched for three biological processes: necrosis, skin diseases, and inflammation. Separate hierarchical clustering was performed using three gene sets, namely 217 genes from the necrosis network (Figure 2), 53 genes from the inflammation network (Figure S6), and 167 genes from the skin diseases network (Figure S7). The clustering analysis in Figure 2 identified four distinct groups of genes (indicated within

yellow borders and labeled as groups A–D in Figure 2), which could be exclusive necrosis markers for TSST-1-L, TSST-1-E, SEA-L, and SEA-E, respectively. This hierarchical analysis failed to mine any exclusive signatures for SEB-E and SEB-L, respectively. Both the inflammation (Figure S6) and the skin diseases (Figure S7) clusters were mined as a single set, each under SEB-L (labelled group A in Figures S6 and S7, respectively). The complete list of all six gene sets is compiled in Table S5.
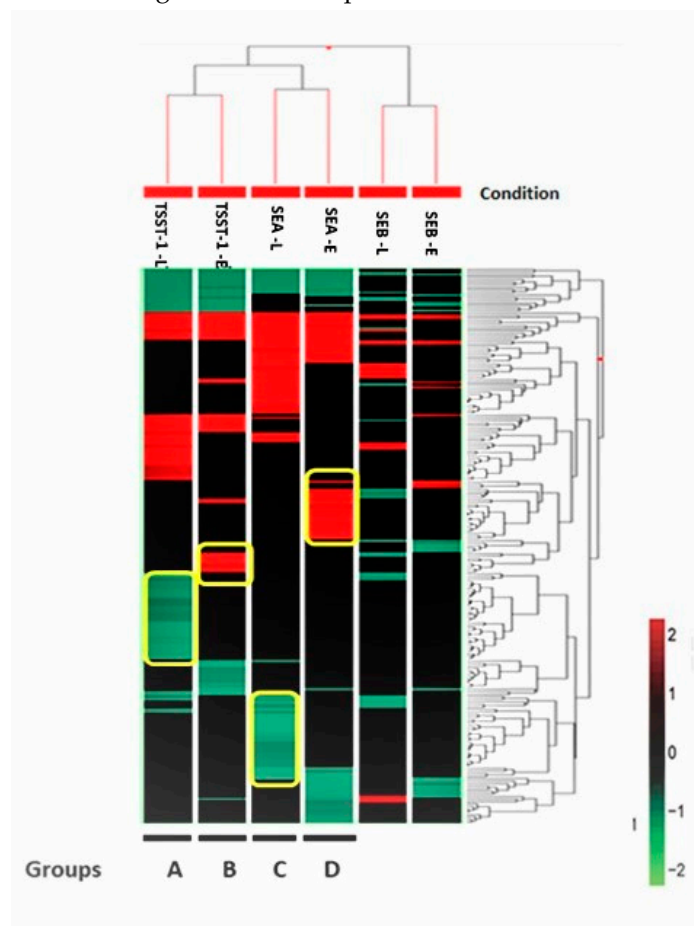

Figure 2. Hierarchical clustering analysis using of 217 genes with a $\log_2$ fold change > |2| enriching the necrosis pathway. The Euclidian algorithm was used to sort both conditions and genes. Each block represents one gene, and its color code is at the bottom right. Clusters bordered by yellow lines represent those genes which were potentially unique signatures of the particular condition. The conditions from left to right are named as TSST-1-L, TSST-1-E, SEA-L, SEA-E, SEB-L, and SEB-E, which represent TSST-1 at the late time point, TSST-1 at the early time point, SEA at the late time point, SEA at the early time point, SEB at the late time point, and SEB at the early time point, respectively.

3.4. Confirmation of Expression Pattern for Select Genes from the Necrosis Clusters

We performed validation of gene expression levels by NanoString nCounter® technology. Table S1 lists the top thirteen highly perturbed genes (up- and downregulated) grouped under necrosis. This list is limited to genes responding only to SEA and TSST-1 for two reasons: first, none of the genes responding in the SEB-E phase were grouped in the three clusters discussed above (Table S5), and second, a lack of sufficient RNA samples for the SEB 48 h treatment point forced us to exclude genes that belong to the SEB-L treatment phase.

Overall, a positive correlation was observed between the NanoString and microarrays results. Of the 13 genes tested, 12 genes followed the same directionality of fold changes for the NanoString and the microarray results (Figure S8) with the exception of one gene (PLCB1).

4. Discussion

The present study investigated in vitro host gene expression patterns induced by SEA, SEB, and TSST-1 during six time points ranging from 0.5 h to 48 h post-toxin exposure. A less frequently tested human skin cell type, but a major component of skin cell-mediated immunology, namely melanocytes, were selected as the target cells. The hybrid character of melanocytes was highlighted as we mined those biofunctions which were linked to the dendritic cell activities and/or the macrophage-based immune responses. This study could have benefited from incorporating additional time points to enhance the resolution of sequential biological events. For instance, our data suggested that the dosages of SEA and TSST-1 used for melanocyte treatments were potentially exhaustive within 24 h p.e.; in this context, extended time points could be highly informative. Furthermore, additional replicates in this study would result in better statistically significant gene identification. To mitigate this drawback to some extent, we mined the networks that met the cut off $p < 0.05$ using hypergeometric tests.

4.1. Distinct Temporal Trend of Pathogenesis Initiated by sAgs

The three toxins SEA, SEB, and TSST-1 of the sAg family are distinct in their structural, functional, and mechanistic properties [7,8,33]. Present literature not only lacks an understanding of molecular pathogenesis underlying the sAgs' toxicity, but also fails to fully comprehend the role of melanocytes in response to sAgs. The melanocytes' dendritic-like nature and their strategic location in the superficial layers of skin qualify them to be excellent mediators of initial immune defense against the sAgs [16–22]. We presented a whole genome-level investigation to compare the melanocytes temporal responses to SEA, SEB, and TSST-1.

A striking observation when comparing SEA and TSST-1 was the similarity in their gene expression patterns across the p.e. time course. Although SEA and TSST-1 share weak overall structural homology, TSST-1 can be displaced by SEA due to shared MHC class II binding sites [33]. This sheds light on the similarities in their mode of action as evidenced by the maximum number of shared networks for both early and late treatment phases.

Compared to SEA and TSST-1, the magnitude of transcriptional response perturbed by SEB was relatively smaller during the early treatment phase. However, the number of genes perturbed by SEB sequentially ramped up. This sort of delayed response is typical for any tissue that is not enriched with lymphocytes, as they are not the direct cellular targets of SEB [14]. Subsequently, SEB caused considerable genomic perturbations between 24 h and 48 h p.e. This trend is to be expected, as SEB typically causes a rapid neutrophil cell death accompanied by vascular congestion and leakage 24 h p.e., causing a shift to a predominantly adaptive immune response [30]. A perturbation in eNOS signalling pathways, potent vasodilators, was reported in the current study.

Another important observation was the temporal differences between SEA- and SEB-induced pathogenesis, particularly during their middle-to-late treatment phases (Figure 1). Nevertheless, a certain cohesiveness emerged between these two sAgs at the functional level. There were 11 and 19 networks that were synchronously enriched by both SEA and SEB at the early and late treatment phases (Figure S3A,B). This fact may demonstrate an underlying similarity in their mode of pathogenesis. Early pathogenesis caused by SEA- and SEB-perturbed genes manifested in skin disorders. In concurrence, SEB exclusively targeted genes linked to T-lymphocytes and their related functions, whereas SEA targeted glucose and protein metabolism networks. The consequences may include dysregulation of immune functions, apoptosis and cell death.

All three toxins enriched several networks related to cell death at early exposure phase and this response continues throughout the time course of the study. This response could be attributed to the moderately high doses of toxins used in the present study. Even though the three toxins perturbed the similar networks during the early exposure phase, as time progressed, each toxin had its unique mode of action in achieving the outcome manifested by cell death and apoptosis. One of the networks that was consistently perturbed by all

three toxins across the p.e. time-course was ILK signalling. ILK functions as a kinase and signal transmitter or as a scaffold protein to facilitate cell–matrix interactions, cell signalling, and cytoskeletal organization [34]. These signals control processes related to survival, proliferation, differentiation, adhesion, migration, contractility, and neovascularization. Inhibition of ILK arrests the cell cycle and promotes apoptosis [35]. This is a key observation to support the following argument.

Early perturbation of genes associated with superoxide radical degradation in SEA indicates an oxidative stress-driven early onset of cell death [36]. TSST also perturbed this mechanism at later time points. Treatment with SEA and TSST down regulated the transcriptional levels of SOD1 and TYRP1, which potentially diminished the synthesis of different isoforms of superoxide dismutase (SODs). The potential loss of SODs highlighted the onset of oxidative stress initiated by the toxins [37], ultimately leading to onset of apoptosis during the late phase p.e.

Additional aspects of the apoptotic network, such as ERK/MAPK, were enriched by SEA and SEB at early p.e. phases, which appears to show a SE-induced apoptotic pathway distinct from that induced by TSST-1 [38,39]. We observed increased expression levels of FOS and NFAT genes during early p.e. SEA and SEB treatments. The FOS gene encodes the proto-oncogene c-FOS protein and NFATs, which are known widely for their cytokine gene expression properties and have been increasingly shown to regulate other genes related to cell cycle progression, cell differentiation, and apoptosis [39,40]. Late phase, SEB p.e. up-regulated genes that encode oncoproteins, such as Rho GTPase, which is also linked with ERK/MAPK [41]. Consequently, the G2/M DNA Damage Checkpoint Regulation, a critical biofunction closely linked with apoptosis, was highly perturbed. At late p.e. phase, SEA cross activated PI3K/AKT signaling, a critical pathway which affects many intracellular processes, including cell survival, growth, and migration.

4.2. Late Phase SEB Is Associated with Certain Dermatological Disorders

sAgs have long been implicated in the development of various inflammatory skin diseases such as psoriasis, atopic dermatitis, Kawasaki Syndrome, etc. [42,43] We observed that all three toxins modulated genes associated with the pathogenesis of psoriasis and chronic psoriasis starting from the early treatment phase. Psoriasis is often associated with functions like cell death, inflammation, autoimmune syndrome, and the production of ROS and nitric oxide [44]. From early to late treatment phases, SEA and TSST-1 shifted the expression of the gene enriching networks that are linked to lichen planus and endometriosis. During the late treatment phase, SEB regulated two unique set of genes that are closely linked to psoriasis and dermatomyositis, respectively. These genes are listed under their respective disease names in Table S3. Concurrent enrichment of oxidative stress networks could be related to the NRF2-mediated oxidative stress response and eNOS signaling pathways. Together these networks typically compromise the host's antioxidant defense mechanisms, a hallmark indicator of psoriasis [45].

4.3. Several Genes of Immunological Networks Are Differentially Modulated by Toxins

The skin exhibits a highly specialized innate immune response to invading pathogens and external stimuli. The major immune players—keratinocytes, Langerhans cells, dendritic cells, resident T-cells, and innate lymphoid cells—act in a coordinated fashion, from sensing the external stimuli to communicating through inflammatory signalling cascades, to ultimately regulating immune homeostasis [46,47]. Accumulating evidence uncovered a hybrid role of melanocytes in regulating innate and adaptive immunity [16–22,24,48–54]. Similar to keratinocytes, melanocytes express several types of toll-like receptors (TLRs) and have the ability to produce several pro-inflammatory cytokines and chemokines [48,52,54]. Melanocytes also regulate the adaptive immunity through their functional similarities to lysosomes, such as capability to phagocytose and their antigen presentation and processing aptitudes [20,48,55]. In this context, we listed those networks (Table 1) which are associated with melanocytes' hybrid role in responding to sAgs.

All of the toxin-induced adaptive immune responses could be attributed to the networks associated with leukocyte (granulocyte/agranulocyte) adhesion, a marker for second tier responses to inflammation induced by infection. Although all toxins contributed to adaptive immunity simulation, the patterns of cytokine production and acute-phase responses differed among the three toxins. For instance, during the early treatment phases of both SEA and SEB, the cytokine and chemokine signalling networks were comprised of CXCL1, CXCL12, and PLCB1, which control leukocyte trafficking; CCL2 and CCL7, which are involved in monocyte migration and macrophage recruitment; and CFL1, which regulates cell morphology and cytoskeletal organization. Early host responses to SEB and TSST-1 included an acute phase response signal that typically triggers non-specific inflammation, leukocytosis, complement activation, protease inhibition, clotting, etc. These responses persisted until 48 h p.e.

All three toxins perturbed IL-17 signalling, a pro-inflammatory signal that bridges innate and adaptive immune responses by playing critical roles in T-cell activation and in promoting the expansion and recruitment of innate immune cells, such as neutrophils [56]. The IL-17 signalling pathway was implicated in response to toxins via alterations of the transcription of several genes in this network, including CXCL1, CXCL5, CXCL8, CCL2, CCL20, and MAP2K6.

5. Conclusions

To our knowledge, this is the first mRNA-level study describing the temporal response of human melanocytes to three staphylococcal superantigenic toxins, namely SEA, SEB, and TSST-1. We observed distinct temporal patterns of transcriptomic regulation for the three individual toxins. The majority of the identified networks were related to necrosis and inflammation, in agreement with previous publications [38–40], although most of the past studies targeted different cells than melanocytes. Pathways related to innate immunity, such as the patterns of cytokine production and acute-phase response, showed toxin-specific regulation. The time-resolved response to SEB assault took a more differential pattern than SEA and TSST-1. In conclusion, these three toxins followed distinguishable pathways to achieve a common endpoint manifested by the cell death coordinated with apoptosis and necrosis. Hence, the temporal knowledge of their pathogenesis could be the key to customized intervention.

Supplementary Materials: The following supporting information can be downloaded at: https://www.mdpi.com/article/10.3390/biomedicines10061402/s1, Figure S1: Temporal profile of overall gene expression patterns in response to SEA: (A) Genes that follow the same expression pattern independent of the treatment time. (B) Genes with altered expression patterns only in one of the two early time points, i.e., 30 min or 2 h post-exposure. (C) Genes with altered expression patterns only toward the end of the exposure period, i.e., either 24 h or 48 h post-exposure; Figure S2: Temporal profile of the overall gene expression patterns in response to SEB: (A) genes that follow the same expression pattern independent of the treatment time. (B) Genes with altered expression patterns only in one of the two early time points, i.e., 30 min or 2 h post-exposure. (C) Genes with altered expression patterns only toward the end of the exposure period, i.e., 48 h post-exposure; Figure S3: Temporal profile of the overall gene expression patterns in response to TSST-1. (A) Genes that follow the same expression pattern independent of the treatment time. (B) Genes with altered expression patterns only in one of the two early time points, i.e., 30 min or 2 h post-exposure. (C) Genes with altered expression patterns only toward the end of the exposure period, i.e., either 24 h or 48 h post-exposure; Figure S4: Number of genes altered in the different experimental conditions. The stacked bar chart shows the number of over-expressed (Fold change > 2) and under-expressed (Fold change < −2) that are marked by black and white color; Figure S5: Venn diagram showing the temporal profiles of non-canonical pathways. (A) Common and unique non-canonical pathways enriched by the three sAgs at Early phases of pathogenesis. For instance, there are 17, 4, and 12 networks which are uniquely perturbed by SEA, SEB, and TSST-1 at early time points. There are 2 networks commonly perturbed by SEA and SEB. Likewise, 19 and 3 networks are commonly perturbed by SEA and TSST-1, and SEB and TSST-1, respectively. There are 9 non-canonical networks that were perturbed by all three sAgs. All of these

networks are listed in the diagram. (B) Common and unique non-canonical pathways enriched by the three sAgs at late phases of pathogenesis. For instance, there are 24, 30 and 3 networks are uniquely perturbed by SEA, SEB and TSST-1 at early time points. There are 10 networks commonly perturbed by SEA and SEB. Likewise, 11 and 0 networks are commonly perturbed by SEA and TSST-1, and SEB and TSST-1, respectively. There are 9 non-canonical networks that were perturbed by all three sAgs. All of these networks are listed in the diagram; Figure S6: Hierarchical clustering analysis using of 53 genes with log2 fold change > |2| enriching the inflammation pathway. Euclidian algorithm is used to sort both conditions and genes. Each block represents one gene, and its color code is at the bottom right. The conditions from left to right are named as TSST-1-L, TSST-1-E, SEA-L, SEA-E, SEB-L and SEB-E, which represent TSST-1-L at late time point, TSST-1-E at early time point, SEA-L at late time point, SEA-E at early time point, SEB-L at late time point and SEB-E at early time point, respectively; Figure S7: Hierarchical clustering analysis using of 167 genes with log2 fold change > |2| enriching the skin disease pathway. The Euclidian algorithm is used to sort both conditions and genes. Each block represents one gene, and its color code is at the bottom right. The conditions from left to right are named as TSST-1-L, TSST-1-E, SEA-L, SEA-E, SEB-L and SEB-E; Figure S8: Targeted gene expression analysis using the NanoString platform to validate the microarray data. Validation study includes a set of 13 genes from three different conditions, namely SEA at early time point, SEA at late time point and TSST-1 at late time point. The color code profile is at the bottom left; Table S1: Top 13 highly perturbed genes grouped under the necrosis cluster; Table S2: Top biological functions and diseases ($p < 0.001$) and canonical functions ($p < 0.01$) identified through IPA for early post-exposure SEA, SEB, and TSST-1 treatments; Table S3: Top biological functions and diseases ($p < 0.001$) and canonical functions ($p < 0.01$) identified through IPA for late post-exposure SEA, SEB, and TSST-1 treatments ($p < 0.001$); Table S4: A list of 36 genes highly perturbed by one of the three sAgs during the early and late post-exposure phases; Table S5: List of significantly different genes that enrich necrosis, inflammation, and the skin diseases pathways, respectively. Genes are sorted by their fold changes, that is, $\log_2$ transformed. The necrosis network is perturbed by TSST-1 at the early (TSST-1-E) and late (TSST-1-L) time points, and SEA at the early (SEA-E) and late (SEA-L) time points. Likewise, networks linked to skin disease and inflammation, respectively, are perturbed by SEB at the late time point (SEB-L).

Disclaimer: Material has been reviewed by the Walter Reed Army Institute of Research. There is no objection to its presentation and/or publication. The opinions or assertions contained herein are the private views of the author, and are not to be construed as official, or as reflecting the true views of the Department of the Army or the Department of Defense.

References

1. Kluytmans, J.; van Belkum, A.; Verbrugh, H. Nasal carriage of Staphylococcus aureus: Epidemiology, underlying mechanisms, and associated risks. *Clin. Microbiol. Rev.* **1997**, *10*, 505–520. [CrossRef] [PubMed]
2. Brown, A.F.; Leech, J.M.; Rogers, T.R.; McLoughlin, R.M. Staphylococcus aureus Colonization: Modulation of Host Immune Response and Impact on Human Vaccine Design. *Front. Immunol.* **2014**, *4*, 507. [CrossRef] [PubMed]
3. Ramarathnam, V.; De Marco, B.; Ortegon, A.; Kemp, D.; Luby, J.; Sreeramoju, P. Risk factors for development of methicillin-resistant Staphylococcus aureus infection among colonized patients. *Am. J. Infect. Control* **2013**, *41*, 625–628. [CrossRef]
4. McKinnell, J.A.; Huang, S.S.; Eells, S.J.; Cui, E.; Miller, L.G. Quantifying the impact of extranasal testing of body sites for methicillin-resistant Staphylococcus aureus colonization at the time of hospital or intensive care unit admission. *Infect. Control Hosp. Epidemiol.* **2013**, *34*, 161–170. [CrossRef] [PubMed]
5. Regenthal, P.; Hansen, J.S.; Andre, I.; Lindkvist-Petersson, K. Thermal stability and structural changes in bacterial toxins responsible for food poisoning. *PLoS ONE* **2017**, *12*, e0172445. [CrossRef]
6. Xu, S.X.; McCormick, J.K. Staphylococcal superantigens in colonization and disease. *Front. Cell. Infect. Microbiol.* **2012**, *2*, 52. [CrossRef]
7. Dinges, M.M.; Orwin, P.M.; Schlievert, P.M. Exotoxins of Staphylococcus aureus. *Clin. Microbiol. Rev.* **2000**, *13*, 16–34. [CrossRef]
8. Pinchuk, I.V.; Beswick, E.J.; Reyes, V.E. Staphylococcal Enterotoxins. *Toxins* **2010**, *2*, 2177–2197. [CrossRef]
9. Fraser, J.; Arcus, V.; Kong, P.; Baker, E.; Proft, T. Superantigens—Powerful modifiers of the immune system. *Mol. Med. Today* **2000**, *6*, 125–132. [CrossRef]
10. Krakauer, T. Immune response to staphylococcal superantigens. *Immunol. Res.* **1999**, *20*, 163–173. [CrossRef]
11. Mendis, C.; Das, R.; Hammamieh, R.; Royaee, A.; Yang, D.; Peel, S.; Jett, M. Transcriptional response signature of human lymphoid cells to staphylococcal enterotoxin B. *Genes Immun.* **2005**, *6*, 84–94. [CrossRef]
12. Vial, T.; Descotes, J. Immune-mediated side-effects of cytokines in humans. *Toxicology* **1995**, *105*, 31–57. [CrossRef]
13. Mattsson, E.; Herwald, H.; Egesten, A. Superantigens from Staphylococcus aureus induce procoagulant activity and monocyte tissue factor expression in whole blood and mononuclear cells via IL-1beta. *J. Thromb. Haemost.* **2003**, *1*, 2569–2576. [CrossRef] [PubMed]
14. Ferreyra, G.A.; Elinoff, J.M.; Demirkale, C.Y.; Starost, M.F.; Buckley, M.; Munson, P.J.; Krakauer, T.; Danner, R.L. Late Multiple Organ Surge in Interferon-Regulated Target Genes Characterizes Staphylococcal Enterotoxin B Lethality. *PLoS ONE* **2014**, *9*, e88756. [CrossRef] [PubMed]
15. Frieri, M.; Capetandes, A. Vascular Endothelial Cell Growth Factor (VEGF) Production by Staphylococcal Enterotoxin B (SEB) and IL-1β-Stimulated Human Keratinocytes is Inhibited by Pimecrolimus. *J. Allergy Clin. Immunol.* **2009**, *123*, S225. [CrossRef]
16. Sulaimon, S.S.; Kitchell, B.E. The biology of melanocytes. *Vet. Dermatol.* **2003**, *14*, 57–65. [CrossRef]
17. Plonka, P.M.; Passeron, T.; Brenner, M.; Tobin, D.J.; Shibahara, S.; Thomas, A.; Slominski, A.L.; Kadekaro, D.; Hershkovitz, E.; Peters, J.J.; et al. What are melanocytes really doing all day long . . . ? *Exp. Dermatol.* **2009**, *18*, 799–819. [CrossRef]
18. Mackintosh, J.A. The antimicrobial properties of melanocytes, melanosomes and melanin and the evolution of black skin. *J. Theor. Biol.* **2001**, *212*, 101–113. [CrossRef]
19. Al Badri, A.M.T.; Todd, P.M.; Garioch, J.J.; Gudgeon, J.E.; Stewart, D.G.; Goudie, R.B. An immunohistological study of cutaneous lymphocytes in vitiligo. *J. Pathol.* **1993**, *170*, 149–155. [CrossRef]
20. Le Poole, I.C.; Mutis, T.; van den Wijngaard, R.M.; Westerhof, W.; Ottenhoff, T.; De Vries, R.R.; Das, P.K. A novel, antigen-presenting function of melanocytes and its possible relationship to hypopigmentary disorders. *J. Immunol.* **1993**, *15*, 7284–7292.
21. Smit, N.; Le Poole, I.; van den Wijngaard, R.; Tigges, A.; Westerhof, W.; Das, P. Expression of different immunological markers by cultured human melanocytes. *Arch. Dermatol. Res.* **1993**, *285*, 356–365. [CrossRef] [PubMed]
22. Lu, Y.; Zhu, W.-Y.; Tan, C.; Yu, G.-H.; Gu, J.-X. Melanocytes are Potential Immunocompetent Cells: Evidence from Recognition of Immunological Characteristics of Cultured Human Melanocytes. *Pigment Cell Res.* **2002**, *15*, 454–460. [CrossRef] [PubMed]
23. Gasque, P.; Jaffar-Bandjee, M.C. The immunology and inflammatory responses of human melanocytes in infectious diseases. *J. Infect.* **2015**, *71*, 413–421. [CrossRef] [PubMed]
24. Tapia, C.V.; Falconer, M.; Tempio, F.; Falcón, F.; López, M.; Fuentes, M.; Alburquenque, C.; Amaro, J.; Bucarey, S.A.; Di Nardo, A. Melanocytes and melanin represent a first line of innate immunity against Candida albicans. *Med. Mycol.* **2014**, *52*, 445–454. [CrossRef] [PubMed]
25. Spaulding, A.R.; Salgado-Pabón, W.; Kohler, P.L.; Horswill, A.R.; Leung, D.Y.M.; Schlievert, P.M. Staphylococcal and Streptococcal Superantigen Exotoxins. *Clin. Microbiol. Rev.* **2013**, *26*, 422–447. [CrossRef] [PubMed]
26. Huber, W.; Carey, V.J.; Gentleman, R.; Anders, S.; Carlson, M.; Carvalho, B.S.; Bravo, H.C.; Davis, S.; Gatto, L.; Girke, T.; et al. Orchestrating high-throughput genomic analysis with Bioconductor. *Nat. Methods* **2015**, *12*, 115–121. [CrossRef] [PubMed]
27. Beard, R.E.; Abate-Daga, D.; Rosati, S.F.; Zheng, Z.; Wunderlich, J.R.; Rosenberg, S.A.; Morgan, R.A. Gene Expression Profiling using Nanostring Digital RNA Counting to Identify Potential Target Antigens for Melanoma Immunotherapy. *Clin. Cancer Res.* **2013**, *19*, 4941–4950. [CrossRef] [PubMed]
28. Veldman-Jones, M.H.; Brant, R.; Rooney, C.; Geh, C.; Emery, H.; Harbron, C.G.; Wappett, M.; Sharpe, A.; Dymond, M.; Barrett, J.C.; et al. Evaluating Robustness and Sensitivity of the NanoString Technologies nCounter Platform to Enable Multiplexed Gene Expression Analysis of Clinical Samples. *Cancer Res.* **2015**, *75*, 2587–2593. [CrossRef]

29. Dauwalder, O.; Thomas, D.; Ferry, T.; Debard, A.-L.; Badiou, C.; Vandenesch, F.; Etienne, J.; Lina, G.; Monneret, G. Comparative inflammatory properties of staphylococcal superantigenic enterotoxins SEA and SEG: Implications for septic shock. *J. Leukoc. Biol.* **2006**, *80*, 753–758. [CrossRef]

30. Bi, S.; Das, R.; Zelazowska, E.; Mani, S.; Neill, R.; Coleman, G.D.; Yang, D.C.; Hammamieh, R.; Shupp, J.W.; Jett, M. The Cellular and Molecular Immune Response of the Weanling Piglet to Staphylococcal Enterotoxin B. *Exp. Biol. Med.* **2009**, *234*, 1305–1315. [CrossRef]

31. Dauwalder, O.; Pachot, A.; Cazalis, M.A.; Paye, M.; Faudot, C.; Badiou, C.; Mougin, B.; Vandenesch, F.; Etienne, J.; Lina, G.; et al. Early kinetics of the transcriptional response of human leukocytes to staphylococcal superantigenic enterotoxins A and G. *Microb. Pathog.* **2009**, *47*, 171–176. [CrossRef]

32. Peterson, M.L.; Ault, K.; Kremer, M.J.; Klingelhutz, A.J.; Davis, C.C.; Squier, C.A.; Schlievert, P.M. The Innate Immune System Is Activated by Stimulation of Vaginal Epithelial Cells with *Staphylococcus aureus* and Toxic Shock Syndrome Toxin 1. *Infect. Immun.* **2005**, *73*, 2164–2174. [CrossRef] [PubMed]

33. Bavari, S.; Ulrich, R.G. Staphylococcal enterotoxin A and toxic shock syndrome toxin compete with CD4 for human major histocompatibility complex class II binding. *Infect. Immun.* **1995**, *63*, 423–429. [CrossRef] [PubMed]

34. Parsons, J.T.; Horwitz, A.R.; Schwartz, M.A. Cell adhesion: Integrating cytoskeletal dynamics and cellular tension. *Nat. Rev. Mol. Cell Biol.* **2010**, *11*, 633–643. [CrossRef] [PubMed]

35. Persad, S.; Attwell, S.; Gray, V.; Delcommenne, M.; Troussard, A.; Sanghera, J.; Dedhar, S. Inhibition of integrin-linked kinase (ILK) suppresses activation of protein kinase B/Akt and induces cell cycle arrest and apoptosis of PTEN-mutant prostate cancer cells. *Proc. Natl. Acad. Sci. USA* **2000**, *97*, 3207–3212. [CrossRef] [PubMed]

36. Nucci, L.A.; Santos, S.S.; Brunialti, M.; Sharma, N.; Machado, F.R.; Assunção, M.; De Azevedo, L.C.P.; Salomao, R. Expression of genes belonging to the interacting TLR cascades, NADPH-oxidase and mitochondrial oxidative phosphorylation in septic patients. *PLoS ONE* **2017**, *12*, e0172024. [CrossRef]

37. Miao, L.; St Clair, D.K. Regulation of superoxide dismutase genes: Implications in disease. *Free Radic. Biol. Med.* **2009**, *47*, 344–356. [CrossRef]

38. Below, S.; Konkel, A.; Zeeck, C.; Müller, C.; Kohler, C.; Engelmann, S.; Hildebrandt, J.-P. Virulence factors of *Staphylococcus aureus* induce Erk-MAP kinase activation and c-Fos expression in S9 and 16HBE14o- human airway epithelial cells. *Am. J. Physiol. Cell. Mol. Physiol.* **2009**, *296*, L470–L479. [CrossRef]

39. Viola, J.P.; Carvalho, L.D.; Fonseca, B.P.; Teixeira, L.K. NFAT transcription factors: From cell cycle to tumor development. *Braz. J. Med. Biol. Res.* **2005**, *38*, 335–344. [CrossRef]

40. Prager, G.; Hadamitzky, M.; Engler, A.; Doenlen, R.; Wirth, T.; Pacheco-Lopez, G.; Krügel, U.; Schedlowski, M.; Engler, H. Amygdaloid Signature of Peripheral Immune Activation by Bacterial Lipopolysaccharide or Staphylococcal Enterotoxin B. *J. Neuroimmune Pharmacol.* **2013**, *8*, 42–50. [CrossRef]

41. Zhang, S.; Han, J.; Sells, M.A.; Chernoff, J.; Knaus, U.G.; Ulevitch, R.J.; Bokoch, G.M. Rho Family GTPases Regulate p38 Mitogen-activated Protein Kinase through the Downstream Mediator Pak1. *J. Biol. Chem.* **1995**, *270*, 23934–23936. [CrossRef]

42. Yarwood, J.M.; Leung, D.Y.; Schlievert, P.M. Evidence for the involvement of bacterial superantigens in psoriasis, atopic dermatitis, and Kawasaki syndrome. *FEMS Microbiol. Lett.* **2000**, *192*, 1–7. [CrossRef]

43. Skov, L.; Baadsgaard, O. Bacterial superantigens and inflammatory skin diseases. *Clin. Exp. Dermatol.* **2000**, *25*, 57–61. [CrossRef] [PubMed]

44. Baz, K.; Cimen, M.B.; Kokturk, A.; Yazici, A.C.; Eskandari, H.G.; Ikizoglu, G.; Api, H.; Atik, U. Oxidant/Antioxidant Status in Patients with Psoriasis. *Yonsei Med. J.* **2003**, *44*, 987–990. [CrossRef]

45. Kadam, D.P.; Suryakar, A.N.; Ankush, R.D.; Kadam, C.Y.; Deshpande, K.H. Role of Oxidative Stress in Various Stages of Psoriasis. *Indian J. Clin. Biochem.* **2010**, *25*, 388–392. [CrossRef]

46. Pasparakis, M.; Haase, I.; Nestle, F.O. Mechanisms regulating skin immunity and inflammation. *Nat. Rev. Immunol.* **2014**, *14*, 289–301. [CrossRef] [PubMed]

47. Elias, P.M. The skin barrier as an innate immune element. *Semin. Immunopathol.* **2007**, *29*, 3–14. [CrossRef]

48. Ahn, J.H.; Park, T.J.; Jin, S.H.; Kang, H.Y. Human melanocytes express functional Toll-like receptor 4. *Exp. Dermatol.* **2008**, *17*, 412–417. [CrossRef] [PubMed]

49. Dessinioti, C.; Stratigos, A.J.; Rigopoulos, D.; Katsambas, A.D. A review of genetic disorders of hypopigmentation: Lessons learned from the biology of melanocytes. *Exp. Dermatol.* **2009**, *18*, 741–749. [CrossRef]

50. Hirobe, T. Structure and function of melanocytes: Microscopic morphology and cell biology of mouse melanocytes in the epidermis and hair follicle. *Histol. Histopathol.* **1995**, *10*, 223–237.

51. Hong, Y.; Song, B.; Chen, H.-D.; Gao, X.-H. Melanocytes and Skin Immunity. *J. Investig. Dermatol. Symp. Proc.* **2015**, *17*, 37–39. [CrossRef] [PubMed]

52. Jin, S.H.; Kang, H.Y. Activation of Toll-like Receptors 1, 2, 4, 5, and 7 on Human Melanocytes Modulate Pigmentation. *Ann. Dermatol.* **2010**, *22*, 486–489. [CrossRef] [PubMed]

53. Kruger-Krasagakes, S.; Krasagakis, K.; Garbe, C.; Diamantstein, T. Production of cytokines by human melanoma cells and melanocytes. *Recent Results Cancer Res.* **1995**, *139*, 155–168.

54. Tam, I.; Stępień, K. Secretion of proinflammatory cytokines by normal human melanocytes in response to lipopolysaccharide. *Acta Biochim. Pol.* **2011**, *58*, 507–511. [CrossRef] [PubMed]

55. Le Poole, I.C.; van den Wijngaard, R.P.; Westerhof, W.; Verkruisen, R.P.; Dutrieux, R.; Dingemans, K.P.; Das, P.K. Phagocytosis by Normal Human Melanocytes In Vitro. *Exp. Cell Res.* **1993**, *205*, 388–395. [CrossRef] [PubMed]
56. Yu, J.J.; Gaffen, S.L. Interleukin-17: A novel inflammatory cytokine that bridges innate and adaptive immunity. *Front. Biosci.* **2008**, *13*, 170–177. [CrossRef]